ACS APPLIED MATERIALS & INTERFACES

Letter

www.acsami.org

Correlating Molecular Structures with Transport Dynamics in High-Efficiency Small-Molecule Organic Photovoltaics

Jiajun Peng,[†] Yani Chen,[†] Xiaohan Wu,[‡] Qian Zhang,[§] Bin Kan,[§] Xiaoqing Chen,[†] Yongsheng Chen,*[,§] Jia Huang,*[,‡] and Ziqi Liang*[,†]

[†]Department of Materials Science, Fudan University, Shanghai 200433, China

[‡]School of Materials Science and Engineering, Tongji University, Shanghai 201804, China

[§]Key Laboratory for Functional Polymer Materials and Centre for Nanoscale Science and Technology, Institute of Polymer Chemistry, College of Chemistry, Nankai University, Tianjin 300071, China

Supporting Information

ABSTRACT: Efficient charge transport is a key step toward high efficiency in small-molecule organic photovoltaics. Here we applied time-of-flight and organic field-effect transistor to complementarily study the influences of molecular structure, trap states, and molecular orientation on charge transport of small-molecule DRCN7T (D1) and its analogue DERHD7T (D2). It is revealed that, despite the subtle difference of the chemical structures, D1 exhibits higher charge mobility, the absence of shallow traps, and better photosensitivity than D2. Moreover, charge transport is favored in the out-of-plane structure within D1-based organic solar cells, while D2 prefers in-plane charge transport.

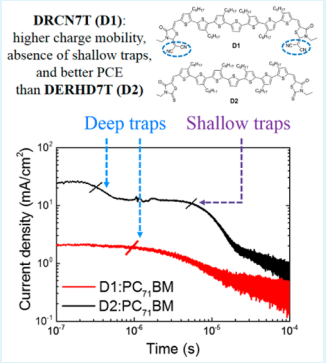

KEYWORDS: *π-conjugated small molecules, organic photovoltaics, transport dynamics, charge mobility, time-of-flight, organic field-effect transistor*

π-Conjugated small molecules are promising solution-processed molecular donors in organic photovoltaic (OPV) cells because of their well-defined molecular structure and molecular weights, facile purification toward mass-scale production, and excellent batch-to-batch reproducibility, which are superior to their polymer analogues.[1−6] These small molecular donors consist of alternating donor (D)−acceptor (A) structures and have recently achieved power conversion efficiencies (PCEs) of up to 10% in a single bulk-heterojunction (BHJ) using a fullerene derivative as the acceptor in the blend.[7,8] Yet, D−A small-molecule-based solar cells commonly suffer from low fill factor (FF) and short-circuit current density (J_{sc}), which often arise from inefficient charge transport and significant charge recombination.[9−11] To resolve those issues, intensive research efforts have been focused on optimization of the blend film morphology,[12−14] but transport dynamics require in-depth investigation.

Charge mobility is an important parameter to quantitatively evaluate the charge-transport process in small-molecule organic solar cells.[15,16] The magnitude of the charge mobility is determined by not only the morphological characteristics of the blend films but also the chemical structures of small molecules.[13,17] Recently, Duzhko et al. found that structural phases and degrees of anisotropy, which were controlled by film fabrication, had a great impact on the charge mobility of high-efficiency donor small molecules.[15] It was concluded that a more isotropic orientation of crystalline domains resulted in higher charge mobility. However, few literature reports have demonstrated how chemical structures of small molecules in high-performance OPV cells influence charge transport.

Here we aim to employ two complementary mobility measurements—time-of-flight (TOF) and organic field-effect transistor (OFET)—to unveil the impact of the molecular structure on the charge-transport dynamics in high-efficiency small-molecule organic solar cells.[18,19] TOF can quantitatively measure the out-of-plane mobilities of both holes and electrons independently while revealing the trap states.[20−23] By contrast, OFET allows one to measure the in-plane hole and electron mobilities of organic semiconductors.[24,25] As a proof-of-concept, we chose two donor small molecules for comparative studies, DRCN7T (denoted as D1) and DERHD7T (denoted as D2),[7] which were recently reported by us and achieved PCEs of 9.30% and 4.35% in BHJ solar cells with a phenyl-C71-butyric acid methyl ester ($PC_{71}BM$) acceptor, respectively.

The molecular structures of D1 and D2 are displayed in Scheme 1. With the same backbone consisting of seven thiophene conjugation units, D1 employs a 2-(1,1-dicyanomethylene)rhodanine to replace the thio group in D2

Received: April 9, 2015
Accepted: June 11, 2015
Published: June 11, 2015

DOI: 10.1021/acsami.5b03073
ACS Appl. Mater. Interfaces 2015, 7, 13137−13141

Scheme 1. Molecular Structures of D1 and D2

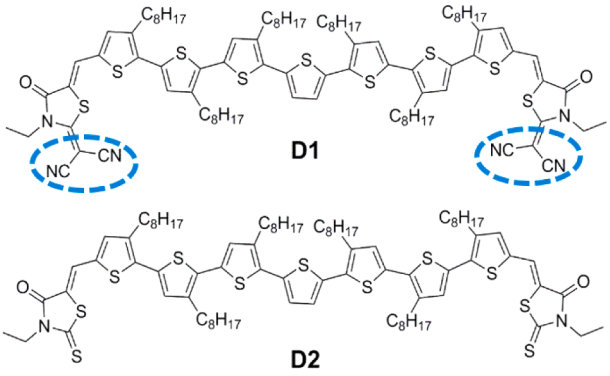

as the terminal unit. Density functional theory (DFT) calculations have suggested that introducing the highly electron-deficient dicyanomethylene group into D1 would increase the ground-state dipole moment and enhance intermolecular electronic coupling, which will therefore reduce the molecular hole reorganization energy.[7] As a result, efficient charge transport in D1-based OPV cells is anticipated. Our goal is to elucidate experimentally why D1 outperforms D2 in organic solar cells through revealing the difference in their charge transport, which leads to strikingly different PCEs. Both TOF and OFET results consistently show that, compared to D2, D1 exhibits the absence of shallow traps and increased light sensitivity. As a consequence, higher hole mobilities are attained in both D1 and its blends with $PC_{71}BM$ than in the D2 counterpart, accounting for its superior photovoltaic performance. Importantly, through comparative mobility measurements in the device architectures of a solar cell and a field-effect transistor, respectively, this work offers a better understanding of how the subtle chemical structures of donor molecules induce remarkably different molecular orientations in thin films and greatly impact the charge-transport dynamics.

Optical absorption spectra were measured as shown in Figure S1 in the Supporting Information (SI), and the obtained optical data are summarized in Table S1 in the SI. The D1 and D2 solutions exhibit bathochromic absorption peaks at 528 and 507 nm, respectively, while both D1 and D2 thin films exhibit a significant red shift in absorption, in which D1 shows a broader and overall stronger absorption than D2. The optical band gap of D1 (1.63 eV) is slightly lower than that of D2 (1.66 eV), which is consistent with the cyclic voltammetry (CV) results (Figure S2 and Table S2 in the SI) in which the electrochemical band gaps of D1 and D2 are 1.60 and 1.65 eV, respectively. Furthermore, a higher photoluminescence (PL) quenching efficiency (91%) is found in the D1:$PC_{71}BM$ blend in comparison to the D2:$PC_{71}BM$ blend (82%), as shown in Figure S3 in the SI.[7]

TOF measurement was then conducted in an organic solar cell structure with a relatively thick active layer (600−800 nm) to ensure that charge carriers traverse the depletion region to attain accurate values of the TOF mobility.[20] Two types of devices were investigated and compared: (i) annealed neat films with device structures of indium−tin oxide (ITO)/poly(3,4-ethylenedioxythiophene):poly(styrenesulfonate) (PEDOT:PSS)/D1 or D2/LiF/Al and (ii) annealed blend films with device architectures of ITO/PEDOT:PSS/D1 or D2 blends with $PC_{71}BM$/LiF/Al. Note that the blend ratio of D1:$PC_{71}BM$ and D2:$PC_{71}BM$ is 1:0.5, which is the optimal ratio to achieve the highest PCE according to our previous report.[7]

We first performed the dark current density versus voltage scans to ensure the good blocking contact created between the electrode and organic films. This is confirmed by Figure S4 in the SI, which shows that the dark current density is much smaller than the following TOF transient current density measured under the laser light. Figure 1 shows the TOF

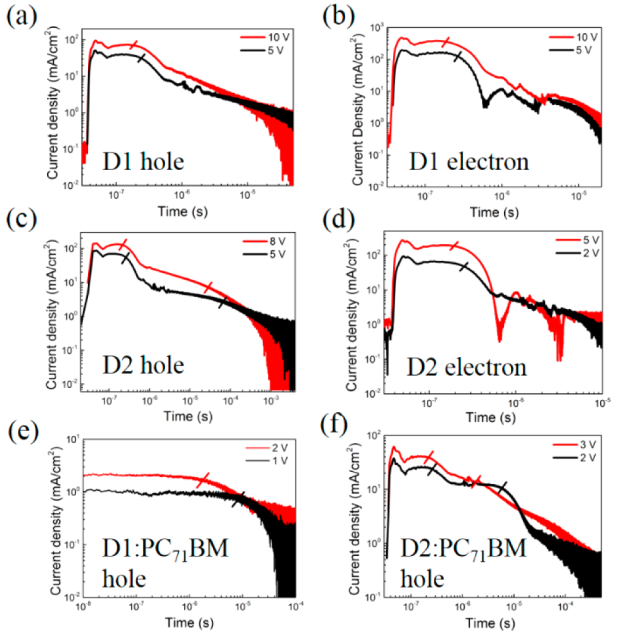

Figure 1. TOF $j-t$ double-logarithmic profiles measured with different applied voltages: (a) hole and (b) electron mobility measurements of an annealed D1 neat film; (c) hole and (d) electron mobility measurements of an annealed D2 neat film; (e) hole mobility measurement of an annealed D1:$PC_{71}BM$ blend film; (f) hole mobility measurement of an annealed D2:$PC_{71}BM$ blend film. Transit times are indicated by the red or black slashes.

transient profiles of photocurrent density (j)−time (t) in a double-logarithmic plot with different applied voltages. The TOF $j-t$ profiles under a linear scale are also presented in Figure S5 in the SI. The slashes in Figures 1 and S5 in the SI highlight the plateau region of the $j-t$ profiles, which determines the transit time (t_{tr}) of charge carriers and the peak number of extracted charge carriers. The mobility of the charge carriers measured by TOF can be calculated from eq 1,[20] where μ is the charge mobility, d is the thickness of the active layer, V is the voltage bias, and t_{tr} is the transient time. The calculated values of the TOF hole and electron mobilities of D1 and D2 are summarized in Table 1.

$$\mu = \frac{d^2}{Vt_{tr}} \quad (1)$$

When the plateau region is formed, it means the photogenerated charge carriers including the trapped ones are extracted, and hence the t_{tr} value can also be used to distinguish the types of trap states.[23] Given the unavoidable impurities and defects introduced in the process of chemical synthesis or device fabrication, trap states including deep or shallow traps exist in the device. The longer t_{tr} results in lower charge mobility, implying that the existence of shallower traps hinders

DOI: 10.1021/acsami.5b03073
ACS Appl. Mater. Interfaces 2015, 7, 13137−13141

Table 1. TOF Results of D1, D2, and Their Blends with $PC_{71}BM$

material	film thickness (nm)	trap type	type of charge carrier	applied voltage (V)	t_{tr} (s)	mobility [$cm^2/(V\ s)$]
D1	800	deep	hole	5.0	2.3×10^{-7}	5.6×10^{-3}
	800	deep	electron		2.6×10^{-7}	4.9×10^{-3}
D2	600	deep	hole	5.0	2.7×10^{-7}	2.7×10^{-3}
	600	shallow	hole		6.5×10^{-5}	1.1×10^{-5}
	600	deep	electron		1.8×10^{-7}	4.1×10^{-3}
D1:$PC_{71}BM$	800	deep	hole	2.0	9.0×10^{-7}	3.5×10^{-3}
D2:$PC_{71}BM$	600	deep	hole	2.0	2.6×10^{-7}	6.9×10^{-3}
	600	shallow	hole		5.8×10^{-6}	3.1×10^{-4}

the charge movement. Likewise, the shorter t_{tr} leads to higher charge mobility.

In a comparison of the $j-t$ profiles of hole mobility measurement, there is only one plateau region in D1 on the time scale of 10^{-7} s (Figure 1a), but there are two plateau regions in D2 on the time scale of 10^{-7} and 10^{-5} s, respectively (Figure 1c). Therefore, the former plateau region on the scale of 10^{-7} s represents the deep traps, while the latter on the scale of 10^{-5} s indicates the shallow traps.[23] Thus, D1 is mainly influenced by deep traps, while D2 is affected by both deep and shallow traps. The charge mobility is remarkably lower if influenced by shallow traps, which cause more circuitous transporting paths than that affected by deep traps. On the other hand, because the activation energy of deep traps is quite large, the trapped carriers are difficult to extract, while the mobile carriers transport with high mobility, close to the intrinsic mobility.[23]

Therefore, as seen from Table 1, the hole and electron mobilities of D1 are 5.6×10^{-3} and 4.9×10^{-3} $cm^2/(V\ s)$, respectively, meaning that excellent and balanced charge transport is achieved in D1. In contrast, both hole and electron mobilities of D2 are notably lower because of the existence of additional shallow traps. Higher hole mobility obtained in D1 coincides well with the DFT prediction upon decreased molecular hole reorganization energy of D1 and the grazing incidence X-ray diffraction (GIXD) results on tight $\pi-\pi$ stacking.[7]

We further applied TOF to study and compare the transport dynamics in the blend films of D1:$PC_{71}BM$ and D2:$PC_{71}BM$. Here we focus on TOF measurements of the hole mobility, which is determined by D1 and D2 donors, while the electron mobility in the blend is dominated by a $PC_{71}BM$ acceptor. Figure 1e represents the double-logarithmic curve to measure the hole mobility in the blend of D1 and $PC_{71}BM$, while Figure 1f represents that of D2 and $PC_{71}BM$. The calculated values of the TOF hole mobilities of the blends of D1 and D2 with $PC_{71}BM$ are summarized in Table 1. As shown in Figure 1e,f, there is only one plateau region representing deep traps in the blend of D1 and $PC_{71}BM$, but there are still two plateau regions representing both deep and shallow traps in the blend of D2 and $PC_{71}BM$. Therefore, the differences of transport dynamics between D1:$PC_{71}BM$ and D2:$PC_{71}BM$ blends are schematically described in Scheme 2. In the D1:$PC_{71}BM$ blend, only deep traps exist, while in the D2:$PC_{71}BM$ blend, there are additional shallow traps, which result in longer transporting paths and more charge recombination prior to charge collection.

To gain deep insight into the transport dynamics, we measured the electric field dependence of hole and electron mobilities at room temperature. Figure 2 shows such dependences of neat films of D1 and D2 and blend films of D1:$PC_{71}BM$ and D2:$PC_{71}BM$. The original TOF double-

Scheme 2. Comparison of the Charge-Transport Dynamics in the Annealed Blend Films of D1 and D2 with $PC_{71}BM$

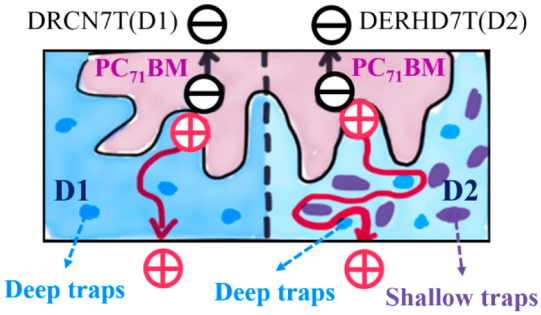

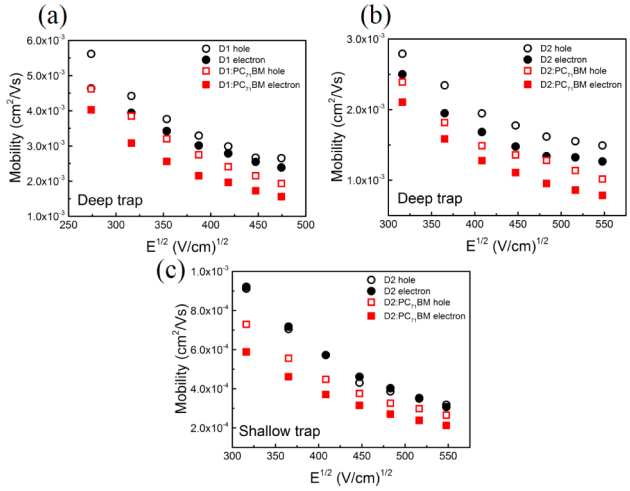

Figure 2. Electric field dependences of the hole and electron mobilities at room temperature: (a) D1 and its blend with $PC_{71}BM$ influenced by deep traps; (b) D2 and its blend with $PC_{71}BM$ influenced by deep traps; (c) D2 and its blend with $PC_{71}BM$ influenced by shallow traps.

logarithmic plots with varying applied voltage from 6 to 18 V are displayed in Figures S6 and S7 in the SI. As shown in Figure 2, both the hole and electron mobilities of D1, D2, and their respective blends with $PC_{71}BM$ all decrease with increasing electric field. Such negative field dependences of the charge mobility at room temperature behavior were also found in other reported high-efficiency small molecules, such as $DTS(FBTTh_2)_2$ and its blend with $PC_{71}BM$.[13,15] Possible explanations were that the positional disorder dominates over the reduced energetic disorder,[15] which could apply to our case.

In addition to out-of-plane TOF measurements, we carried out OFET measurements to study the in-plane charge transport of D1 and D2. Figures 3 and 4 show the output characteristics (drain current versus drain-to-source voltage, $I_{SD}-V_{SD}$) and transfer characteristics (drain current versus gate-to-source

DOI: 10.1021/acsami.5b03073
ACS Appl. Mater. Interfaces 2015, 7, 13137−13141

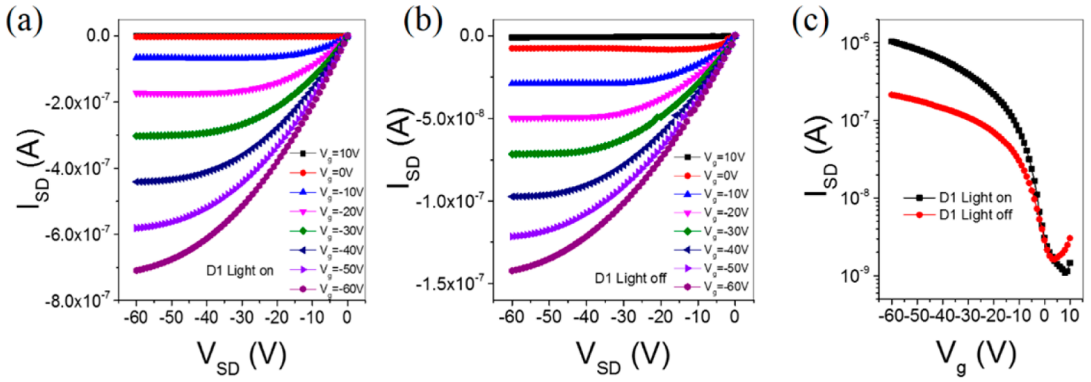

Figure 3. Field-effect transistor performance of D1: output characteristics with (a) light on and (b) light off; (c) transfer characteristics with light on and off.

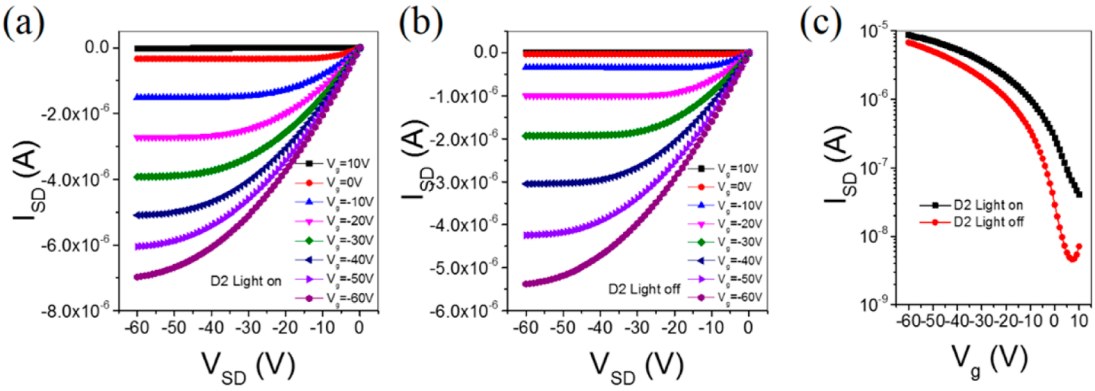

Figure 4. Field-effect transistor performance of D2: output characteristics of D2 with (a) light on and (b) light off; (c) transfer characteristics with light on and off.

voltage, $I_{SD}-V_g$) of OFETs based on D1 and D2, in the dark and under a white-light illumination of 7 mW/cm^2. All devices exhibit p-type transistor characteristics with clear linear and saturation regions. The D1 OFET shows a saturation drain current 1 order of magnitude lower than that of the D2 OFET. However, the D1 device is more sensitive to light than the D2 device. As shown in Figure 3, in the dark D1 exhibits an effective field-effect hole mobility $\mu_{\text{dark-D1}} = 2.8 \times 10^{-4}$ cm^2/(V s) and under light illumination $\mu_{\text{light-D1}} = 2.3 \times 10^{-3}$ cm^2/(V s), which is 8 times higher than $\mu_{\text{dark-D1}}$. In contrast, as shown in Figure 4, D2 exhibits a higher effective hole mobility [$\mu_{\text{dark-D2}} = 1.62 \times 10^{-2}$ cm^2/(V s) and $\mu_{\text{light-D2}} = 1.66 \times 10^{-2}$ cm^2/(V s)]. Under light illumination, the current density increases more obviously in D1 than D2, as shown in Figures 2c and 3c, suggesting that D1 is more photosensitive than D2. The higher photosensitivity of D1 than D2 also coincides with the UV−vis and TOF results in which D1 exhibits a broader and stronger absorption spectrum and less charge recombination caused by reduced traps than D2.

These OFET results are, however, in sharp contrast to our TOF results in which the hole mobility of D1 is significantly higher than that of D2. This indeed originates from the preferred direction of charge transport due to different device configurations. The OFET results that measure in-plane charge transport coincide with the GIXD results in which D2 prefers the edge-on orientation normal to the surface of the films while D1 shows more prominent face-on orientations,[7] which agrees with the TOF results in which the hole mobility of D1 is higher than that of D2 in out-of-plane structures.

In conclusion, we have performed comparative studies on D1 and its analogue D2 to unravel the impact of chemical structures on the transport dynamics. By combining TOF and OFET techniques, we demonstrated that charge transport was favored in the out-of-plane OPV structure of D1 because of its absence of shallow traps while D2 preferred the in-plane charge transport, which agrees with the difference of molecular orientations, as previously suggested by GIXD results. In addition, D1 was found to be more photosensitive than D2. This study offers a detailed dynamic investigation of high-efficiency small-molecule organic solar cells.

■ ASSOCIATED CONTENT

Supporting Information

Materials and methods, optical absorption spectra, CV, PL spectra, dark current density versus voltage ($J-V$) curves of TOF devices, TOF $j-t$ linear-scale profiles measured with different applied voltages, and original TOF double-logarithmic plots for studying the electric field dependence of hole and electron mobilities. The Supporting Information is available free of charge on the ACS Publications website at DOI: 10.1021/acsami.5b03073.

■ AUTHOR INFORMATION

Corresponding Authors

*E-mail: yschen99@nankai.edu.cn.
*E-mail: huangjia@tongji.edu.cn.
*E-mail: zqliang@fudan.edu.cn.

DOI: 10.1021/acsami.5b03073
ACS Appl. Mater. Interfaces 2015, 7, 13137−13141

Notes

The authors declare no competing financial interest.

■ ACKNOWLEDGMENTS

Z.L. acknowledges support of the National Natural Science Foundation of China (NSFC) under Grant 51473036. J.H. is thankful for support of the NSFC under Grants 51373123 and 21302142.

■ REFERENCES

(1) Roncali, J.; Leriche, P.; Blanchard, P. Molecular Materials for Organic Photovoltaics: Small is Beautiful. *Adv. Mater.* **2014**, *26*, 3821−3838.
(2) Coughlin, J. E.; Henson, Z. B.; Welch, G. C.; Bazan, G. C. Design and Synthesis of Molecular Donors for Solution-Processed High-Efficiency Organic Solar Cells. *Acc. Chem. Res.* **2014**, *47*, 257−270.
(3) Chen, Y.; Wan, X.; Long, G. High Performance Photovoltaic Applications Using Solution-Processed Small Molecules. *Acc. Chem. Res.* **2013**, *46*, 2645−2655.
(4) Mishra, A.; Bäuerle, P. Small Molecule Organic Semiconductors on the Move: Promises for Future Solar Energy Technology. *Angew. Chem., Int. Ed.* **2012**, *51*, 2020−2067.
(5) Lin, Y.; Li, Y.; Zhan, X. Small Molecule Semiconductors for High-Efficiency Organic Photovoltaics. *Chem. Soc. Rev.* **2012**, *41*, 4245−4272.
(6) Walker, B.; Kim, C.; Nguyen, T.-Q. Small Molecule Solution-Processed Bulk Heterojunction Solar Cells. *Chem. Mater.* **2011**, *23*, 470−482.
(7) Zhang, Q.; Kan, B.; Liu, F.; Long, G.; Wan, X.; Chen, X.; Zuo, Y.; Ni, W.; Zhang, H.; Li, M.; Hu, Z.; Huang, F.; Cao, Y.; Liang, Z.; Zhang, M.; Russell, T. P.; Chen, Y. Small-Molecule-Based Solar Cells with Efficiency over 9%. *Nat. Photonics* **2015**, *9*, 35−41.
(8) Kan, B.; Zhang, Q.; Li, M.; Wan, X.; Ni, W.; Long, G.; Wang, Y.; Yang, X.; Feng, H.; Chen, Y. Solution-Processed Organic Solar Cells Based on Dialkylthiol-Substituted Benzodithiophene Unit with Efficiency near 10%. *J. Am. Chem. Soc.* **2014**, *136*, 15529−15532.
(9) Zhang, Y.; Dang, X.-D.; Kim, C.; Nguyen, T.-Q. Effect of Charge Recombination on the Fill Factor of Small Molecule Bulk Heterojunction Solar Cells. *Adv. Energy Mater.* **2011**, *1*, 610−617.
(10) Kyaw, A. K. K.; Wang, D. H.; Tseng, H.-R.; Zhang, J.; Bazan, G. C.; Heeger, A. J. Electron and Hole Mobility in Solution-Processed Small Molecule−Fullerene Blend: Dependence on the Fullerene Content. *Appl. Phys. Lett.* **2013**, *102*, 163308.
(11) Li, Z.; Lin, J. D. A.; Phan, H.; Sharenko, A.; Proctor, C. M.; Zalar, P.; Chen, Z.; Facchetti, A.; Nguyen, T.-Q. Competitive Absorption and Inefficient Exciton Harvesting: Lessons Learned from Bulk Heterojunction Organic Photovoltaics Utilizing the Polymer Acceptor P(NDI2OD-T2). *Adv. Funct. Mater.* **2014**, *24*, 6989−6998.
(12) Kyaw, A. K. K.; Wang, D. H.; Luo, C.; Cao, Y.; Nguyen, T.-Q.; Bazan, G. C.; Heeger, A. J. Effects of Solvent Additives on Morphology, Charge Generation, Transport, and Recombination in Solution-Processed Small-Molecule Solar Cells. *Adv. Energy Mater.* **2014**, *4*, 1301469.
(13) Proctor, C. M.; Albrecht, S.; Kuik, M.; Neher, D.; Nguyen, T.-Q. Overcoming Geminate Recombination and Enhancing Extraction in Solution-Processed Small Molecule Solar Cells. *Adv. Energy Mater.* **2014**, *4*, 1400230.
(14) Zalar, P.; Kuik, M.; Ran, N. A.; Love, J. A.; Nguyen, T.-Q. Effects of Processing Conditions on the Recombination Reduction in Small Molecule Bulk Heterojunction Solar Cells. *Adv. Energy Mater.* **2014**, *4*, 1400438.
(15) Karak, S.; Liu, F.; Russell, T. P.; Duzhko, V. V. Bulk Charge Carrier Transport in Push−Pull Type Organic Semiconductor. *ACS Appl. Mater. Interfaces* **2014**, *6*, 20904−20912.
(16) Proctor, C. M.; Love, J. A.; Nguyen, T.-Q. Mobility Guidelines for High Fill Factor Solution-Processed Small Molecule Solar Cells. *Adv. Mater.* **2014**, *26*, 5957−5961.
(17) Proctor, C. M.; Kim, C.; Neher, D.; Nguyen, T.-Q. Nongeminate Recombination and Charge Transport Limitations in Diketopyrrolopyrrole-Based Solution-Processed Small Molecule Solar Cells. *Adv. Funct. Mater.* **2013**, *23*, 3584−3594.
(18) Mozer, A. J.; Sariciftci, N. S.; Pivrikas, A.; Österbacka, R.; Juška, G.; Brassat, L.; Bässler, H. *Phys. Rev. B* **2005**, *71*, 035214.
(19) Camaioni, N.; Tinti, F.; Esposti, A. D.; Righi, S.; Usluer, O.; Boudiba, S.; Egbe, D. A. M. Electron and Hole Transport in an Anthracene-Based Conjugated Polymer. *Appl. Phys. Lett.* **2012**, *101*, 053302.
(20) Tiwari, S.; Greenham, N. C. Charge Mobility Measurement Techniques in Organic Semiconductors. *Opt. Quantum Electron.* **2009**, *41*, 69−89.
(21) Liu, C.-Y.; Chen, S.-A. Charge Mobility and Charge Traps in Conjugated Polymers. *Macromol. Rapid Commun.* **2007**, *28*, 1743−1760.
(22) Laquai, F.; Wegner, G.; Bässler, H. What Determines the Mobility of Charge Carriers in Conjugated Polymers? *Philos. Trans. R. Soc., A* **2007**, *365*, 1473−1487.
(23) Li, C.; Duan, L.; Li, H.; Qiu, Y. Universal Trap Effect in Carrier Transport of Disordered Organic Semiconductors: Transition from Shallow Trapping to Deep Trapping. *J. Phys. Chem. C* **2014**, *118*, 10651−10660.
(24) Bao, Z.; Dodabalapur, A.; Lovinger, A. J. Effect of Mesoscale Crystalline Structure on the Field-Effect Mobility of Regioregular Poly(3-hexylthiophene) in Thin-Film Transistor. *Appl. Phys. Lett.* **1996**, *69*, 4108−4110.
(25) Wei, Q.; Hashimoto, K.; Tajima, K. Experimental Investigation of Charge Carrier Transport in Organic Thin-Film Transistors with "Buried Surface Layers". *ACS Appl. Mater. Interfaces* **2011**, *3*, 139−142.

DOI: 10.1021/acsami.5b03073
ACS Appl. Mater. Interfaces 2015, 7, 13137−13141